IEEE Access
Multidisciplinary | Rapid Review | Open Access Journal

Received 6 October 2022, accepted 2 November 2022, date of publication 14 November 2022, date of current version 17 November 2022.

Digital Object Identifier 10.1109/ACCESS.2022.3221987

RESEARCH ARTICLE

Hybrid Predistorter for Broadband Power Amplifiers Linearization With Relaxed DAC Speed in the Signal Transmit Path

ANFAL ALSAYED ALI, SERIEN AHMED, AND OUALID HAMMI, (Member, IEEE)
Department of Electrical Engineering, American University of Sharjah, Sharjah, United Arab Emirates

Corresponding author: Oualid Hammi (ohammi@aus.edu)

This work was supported in part by the Research Office at the American University of Sharjah under Grant FRG20-M-E85, and in part by the Open Access Program from the American University of Sharjah.

ABSTRACT This paper proposes a novel predistorter architecture suitable for hybrid baseband/RF implementation. The distortion function is split into a memory polynomial and an AM/AM only look-up table (LUT). The memory polynomial function is to be applied in the baseband digital domain whereas the LUT predistorter is suitable for low complexity implementation in either the baseband digital or the RF analog domains. The proposed model was compared to benchmark models using 20MHz and 40MHz wide 5G test signals, and found to be superior in terms of adjacent channel leakage ratio performance and complexity. Experimental results showed that the model can achieve ACLR levels of better than −50dBC with a relatively low number of coefficients. The proposed model requires around 20% less coefficients than the reverse twin-nonlinear two-box model, and achieves slightly better ACLR while easing the analog implementation of the static nonlinearity predistortion function. Most importantly, the low-complexity hybrid implementation of the proposed model can drastically reduce the speed requirements in the digital to analog converter of the signal transmit path by up to 80% when compared to traditional DPD systems.

INDEX TERMS Broadband, digital predistortion, distortions, memory effects, memory polynomial, nonlinearity, power amplifier, RF predistortion.

I. INTRODUCTION

Modern communication systems are prone to the unavoidable nonlinear distortions caused by the radio frequency (RF) front-end and more specifically the RF power amplifier (PA). These distortions emanate from the use of amplitude modulated signals, for spectral efficiency and data throughput considerations, and from the need for power-efficient amplification systems. To meet spectrum emission constraints set by the communication standards, mitigation of nonlinear distortions is a vital aspect in wireless transmitters [1], [2], [3], [4].

Baseband digital predistortion commonly referred to as digital predistortion (DPD) has been the preferred linearization technique in wireless communication infrastructure for the last two decades. This is mainly due to the benefits of the digital implementation which allows for the accurate synthesis of the predistortion function. In fact, to compensate for PAs' dynamic nonlinear behavior (which includes static nonlinearity and memory effects), a wide range of predistortion functions have been proposed in the literature. These include memory polynomial based functions [5], [6], [7], two-box functions [8], [9], [10], and neural networks [11], [12], [13], [14]. The development of novel predistortion function is certainly the area that received most of the interest from the research community actively working on predistortion systems. However, there are a few other key factors that influence the performance of digital predistortion systems. These factors are becoming increasingly important in the context of 5G communication systems in which broadband transmission bandwidths are needed. For example, the maximum channel bandwidth defined for the first frequency range (FR1) in 5G is 100MHz, whereas the channel bandwidth can reach

The associate editor coordinating the review of this manuscript and approving it for publication was Vittorio Camarchia.

This work is licensed under a Creative Commons Attribution 4.0 License. For more information, see https://creativecommons.org/licenses/by/4.0/

up to 400MHz in the second frequency range (FR2) also known as mmWaves [15]. The bandwidth of the signals being transmitted have three major effects on digital predistortion systems. Firstly, power amplifiers distortions cause spectral regrowth at the PA output which translates into an output signal bandwidth that is typically five times that of the signal to be transmitted. This requires high speed analog to digital converters (ADC) in the feedback path used to acquire the PA output signal which will be used to derive the predistortion function. Several attempts have been made in the literature to address this issue [16], [17], [18]. Secondly, the broad bandwidth of the signals causes the amplifier to exhibit stronger memory effects, and hence calls for more advanced PA and DPD models. Thirdly, the predistortion function, which is inherently a nonlinear function complementary to that of the power amplifier, also results in a spectrum regrowth causing the predistorted signal bandwidth to be comparable to that at the amplifier's output, that is five times the bandwidth of the signal to be transmitted. This sets stringent requirement on the digital to analog converter (DAC) in the signal transmit path. In this paper, we focus on this latter aspect, and propose a novel low-complexity predistortion technique suitable for hybrid baseband-digital/RF-analog implementation. Such implementation is highly attractive for lower power PAs such as cell phones or femtocells base stations. This has the potential to significantly alleviate the speed requirements on the digital to analog converter in the transmit path of digital predistortion systems. In section II, the proposed digital predistortion technique is introduced and compared to existing alternatives. The experimental setup used to validate the proposed DPD is presented in Section III along with its linearization performance. The relaxed DAC speed that can achieved by the proposed hybrid DPD is demonstrated in section IV. Finally, the conclusions of this work are summarized in Section V.

II. PROPOSED PREDISTORTER

In this section, the proposed digital predistorter is discussed from two aspects. First, the proposed predistortion function is introduced. Then, its possible implementations are discussed.

A. PROPOSED PREDISTORTION FUNCTION

Digital predistortion systems are typically implemented in baseband. This allows for taking full benefits of the digital domain implementation. Hence, making it possible to implement sophisticated predistortion functions that can satisfactorily compensate for the distortions of highly nonlinear power amplifiers exhibiting memory effects. The main drawback of this technique is the need to process a predistorted signal that typically has five times the bandwidth of the original input signal. Several attempts have been made to address this issue and implement the predistortion function in the RF domain. However, the RF predistorters reported are mainly memoryless and hence not suitable for modern applications [19], [20], [21]. The envelope memory polynomial (EMP) predistorter is suitable for RF digital implementation [7], [22]. This model compensates for static distortions but has limited performance in the presence of strong memory effects. Other models that can be considered as suitable candidates for RF digital predistortion are the nested look-up tables based predistorters [23], [24]. However, these typically require extensive processing to synthesize the nested LUT which usually has a very large size.

The hybrid predistortion function proposed in this work consists of two sub-functions, and is inspired from the reverse twin-nonlinear two-box (RTNTB) model [8]. The RTNTB model, illustrated in Fig. 1, is made of the cascade of a memory polynomial function followed by a memoryless predistortion function. The two-box implementation of the predistortion function allows for the use of a highly nonlinear memoryless function and a mildly nonlinear dynamic function. This has been found to outperform the conventional memory polynomial model while significantly reducing the model complexity (total number of coefficients) [8]. The memoryless nonlinear function can be implemented either analytically as a memoryless polynomial or as a look-up table. The use of a look-up table circumvents the need to identify highly nonlinear polynomial functions which are often associated with ill-conditioned matrices inversion. In the two box-configuration, the memory polynomial function is often mildly nonlinear and hence is not associated with ill-conditioned matrices.

The two predistortion sub-functions of the RTNTB model are derived sequentially. First, the memoryless nonlinear function is identified. Second, the measured data is de-embedded to derive the input and output waveforms of the memory polynomial function. Finally, the coefficients of the memory polynomial predistortion function are calculated.

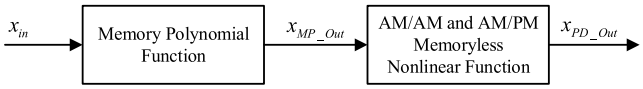

FIGURE 1. Block diagram of the RTNTB predistorter.

The intermediate predistorted signal obtained at the output of the MP sub-model is given by

$$x_{MP\_Out}(n) = \sum_{i=1}^{N} \sum_{j=0}^{M} a_{ij} \cdot x_{in}(n-j) \cdot |x_{in}(n-j)|^{i-1} \quad (1)$$

where $x_{in}(n)$ and $x_{MP\_Out}(n)$ are the n^{th} samples of the memory polynomial's predistortion function input and output waveforms, respectively. a_{ij} are the complex-valued coefficients of the model. N and M are the memory polynomial function's nonlinearity order and memory depth, respectively.

When the memoryless nonlinear function is implemented as a complex-gain power dependent LUT, the n^{th} sample of the predistorter's output $x_{PD\_out}(n)$ will be given by:

$$x_{PD\_out}(n) = G_{LUT}\left(\left|x_{MP\_Out}(n)\right|\right) \cdot x_{MP\_Out}(n) \quad (2)$$

where G_{LUT} is a complex-valued power dependent gain that corresponds to the AM/AM and AM/PM predistortion functions implemented within the LUT.

When the memoryless nonlinear function is implemented as a memoryless polynomial, the predistorter's output (x_{PD_out}) will be related to the x_{MP_Out} through

$$x_{PD\_out}(n) = \sum_{k=1}^{K} b_k \cdot x_{MP\_Out}(n) \cdot \left|x_{MP\_Out}(n)\right|^{k-1} \quad (3)$$

where K and b_k are the nonlinearity order and the complex-valued coefficients of the memoryless polynomial function, respectively.

The proposed predistorter consists of a memory polynomial followed by an AM/AM only memoryless predistortion function as depicted in Fig. 2. The main difference compared to the RTNTB model is that the memoryless nonlinear function used in the proposed predistorter only compensates for the AM/AM distortions and does not include any AM/PM compensation. This is a major aspect that will reduce the complexity of the proposed predistorter and facilitate its implementation in a hybrid architecture.

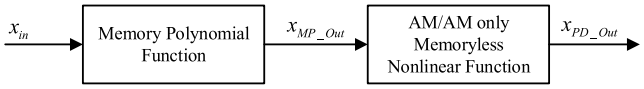

FIGURE 2. Block diagram of the proposed predistorter.

In the proposed model, the intermediate predistorted signal (x_{MP_Out}) is related to the input signal (x_{in}) according to the generic memory polynomial function expressed in Eq. (1). The predistorter output (x_{PD_out}) obtained after passing the intermediate predistorted signal (x_{MP_Out}) through the AM/AM only memoryless function can be expressed according to Eq. (2) or Eq. (3) depending on whether the memoryless predistortion function is implemented as a LUT or as a polynomial function, respectively. However, in both cases, the model parameters of the memoryless function will become real-valued. In fact, when the memoryless predistortion function is implemented as a LUT in the proposed model, the complex-valued power dependent gain will be reduced to a simple real-valued power dependent gain. Similarly, if the memoryless predistortion function is implemented as a memoryless polynomial function, the proposed predistorter will only require real-valued coefficients in contrast with the complex-valued coefficients needed for this sub-block in the conventional RTNTB model.

The identification of the proposed DPD parameters is performed sequentially. From the measured input and output data, the AM/AM LUT is first identified. Then, the signals at the input and output of the memory polynomial function are obtained by de-embedding the measured data. The resulting signals representing the input and output of the memory polynomial function are then used to identify the coefficients of the memory polynomial sub-block of the proposed DPD.

B. IMPLEMENTATIONS OF THE PROPOSED PREDISTORTION FUNCTION

The proposed predistortion function can be implemented fully in the baseband digital domain as illustrated in Fig. 3. In this case, it is conceptually similar to the RTNTB model but presents a complexity reduction related to the identification of the predistortion function. In fact, the AM/AM only LUT used in the proposed predistorter has 50% less complexity when compared to the AM/AM and AM/PM LUT used in the RTNTB predistorter. Indeed, rather than identifying a complex gain that has a magnitude and phase, the LUT sub-function in the proposed model only applies an AM/AM predistortion function. The AM/PM corrections are set to 0 for all input power values. Hence, no identification of the LUT's AM/PM function is needed. By requiring only real-valued coefficients rather than complex-valued coefficients, the identification and implementation of this sub-block will result in 50% less complexity than its counterpart in the RTNTB predistorter.

FIGURE 3. Baseband digital implementation of the proposed predistorter.

A more advantageous implementation of the proposed model is depicted in Fig. 4. In this hybrid implementation, the memory polynomial function is implemented in the digital domain, while the look-up table based AM/AM predistortion function is implemented in the RF analog domain. It is worth pointing out that the hybrid implementation is also possible for the case of the RTNTB predistorter. However, this would require the implementation of the complex-gain memoryless predistortion function in the analog domain. Such implementation is tedious but has been successfully reported. In the case of the proposed DPD, the implementation in the analog domain is made simpler since it is limited to an AM/AM function and does not require any AM/PM compensation.

FIGURE 4. Hybrid implementation of the proposed predistorter.

In this hybrid implementation, only the weakly nonlinear MP function is implemented in the baseband digital domain. Hence, the partly predistorted signal (x_{MP_Out}) being fed into the digital-to-analog converter is expected to have much narrower bandwidth than the fully predistorted signal (x_{PD_Out}). Therefore, alleviating stringent speed requirements. This aspect will be discussed in Section IV.

III. EXPERIMENTAL VALIDATION

The performances of the proposed predistorter were validated experimentally and benchmarked against the RTNTB model and the EMP model. The envelope memory polynomial model is expressed according to:

$$x_{EMP\_out}(n) = \sum_{i=1}^{N}\sum_{j=0}^{M} a_{ij} \cdot x_{in}(n) \cdot \left|x_{in}(n-j)\right|^{i-1} \quad (4)$$

where $x_{in}(n)$ and $x_{EMP\_out}(n)$ are the n^{th} samples of the input and output waveforms of the EMP predistorter, respectively.

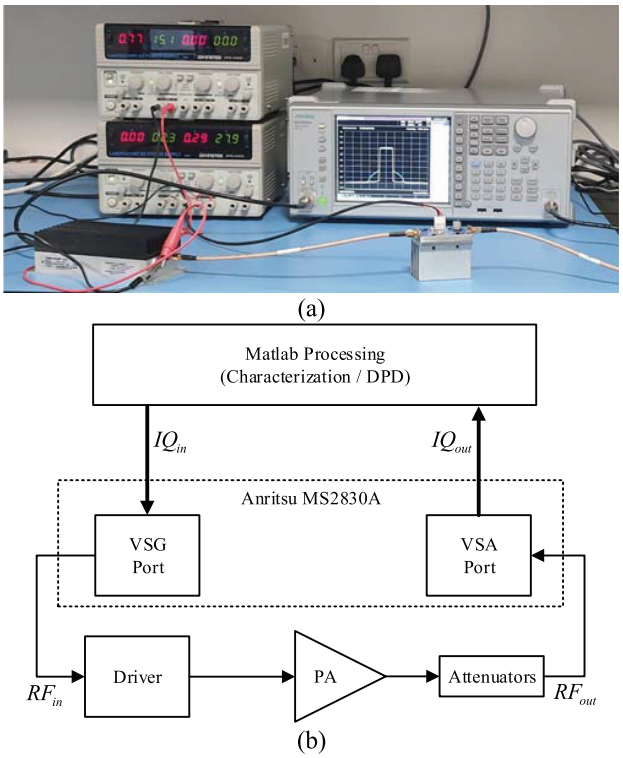

FIGURE 5. Experimental setup for PA characterization and predistortion (a) Photograph of the experimental setup, (b) Simplified block diagram of the experimental setup.

N and M are the nonlinearity order and the memory depth of the EMP function, respectively. a_{ij} are the complex-valued model coefficients. The EMP model is selected for benchmarking since it is one of the few models that are able to compensate for memory effects while being suitable for implementation in the RF analog domain [7].

The device under test (DUT) used in this experimental validation is a commercial GaN based class AB amplifier CGH40010-AMP from Wolfspeed Inc. The setup consists of a vector signal generator (VSG) and a vector signal analyzer (VSA) pair used to drive the power amplifiers lineup made of a driver (ZHL-42 from Mini-Circuits) and the DUT. The experimental setup is presented in Fig. 5. Anritsu MS2830A was used in this work. It incorporates both the VSG and VSA functions within the same instrument. The resolution of the VSG was 16 bits, while that of the VSA was 14 bits.

The DUT was driven by two 5G test signals with bandwidths of 20MHz and 40MHz, respectively. The sampling rate of the test signals were set to 122.88Msps and 153.6Msps for the 20MHz and the 40MHz signals, respectively. Both signals have a duration of 1ms. This corresponds to 122880 samples for the 20MHz waveform, and 153600 samples for the 40MHz test signal. The measured AM/AM and AM/PM characteristics of the DUT when driven by the 20MHz test signal are reported in Fig. 6. This figure shows the extent of the nonlinear distortions and memory effects exhibited by the DUT. The small signal gain of the DUT is 12dB. In all experiments, the DUT was operated at an output power

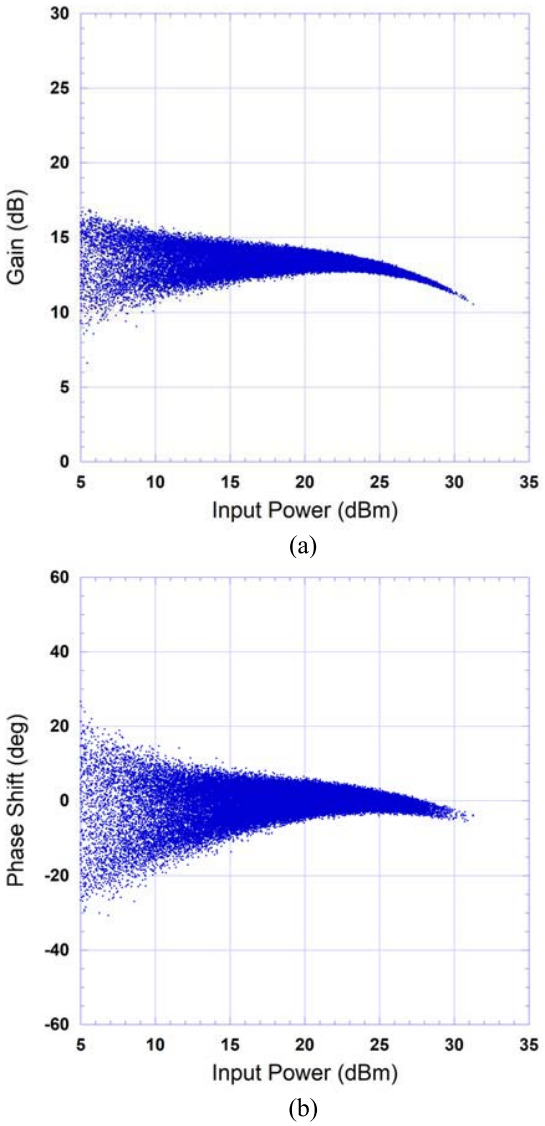

FIGURE 6. Measured gain characteristics of the DUT (a) AM/AM Characteristic, (b) AM/PM Characteristic.

back-off equal to the signal's PAPR (10.9dB) to ensure that it is driven over its entire power range. This corresponds to an average output power of 32dBm and an average drain efficiency of 24%.

In this work, the indirect learning architecture was used to identify all predistortion functions. This allows for the extraction of the DPD coefficients without the need to identify a PA model. The identification of the DPD coefficients was performed using only 8,000 samples of the measured data. The full waveform was used for the validation and performance assessment including normalized mean squared error (NMSE) calculation and PA linearization. The coefficients of the polynomial functions were derived using the least squares algorithm.

To assess the performance of the proposed predistorter, two benchmark models were considered. The first benchmark model is the RTNTB model which is comparable to the

proposed model in the sense that it is made of a MP function followed by a LUT. Comparing the proposed model to the RTNTB model will demonstrate if there is any loss of performance in the proposed model due to the use a real-valued AM/AM only LUT rather than a complex-valued AM/AM and AM/PM LUT. The second model against which the performance of the proposed model is benchmarked is the EMP model. The main reason behind this comparison is to relate the performance of the proposed model to another model that compensates for memory effects and can be implemented either in baseband digital or in the RF analog domains similar to the proposed model.

First, the DUT was characterized and the measured input and output waveforms were used to synthesize the LUT functions of the RTNTB and the proposed DPD. Then, the measured waveforms were de-embedded to obtain the input and output signals of the memory polynomial sub-model in the RTNTB and the proposed predistorters. Using these signals, the nonlinearity order and the memory depth of the memory polynomial function in each DPD were varied. The nonlinearity order was swept from 1 to 7, and the memory depth was varied from 1 to 5. For each pair of values (nonlinearity order and memory depth), a predistorter was synthesized and applied to linearize the DUT. First, the DPD accuracy was assessed by calculating the normalized mean squared error between the desired DPD output and the actual DPD output as a function of the memory polynomial's number of coefficients. The memory polynomial size $\left(Size_{Poly}\right)$ corresponds to the number of complex-valued coefficients, and is given by:

$$Size_{Poly} = N \cdot (M + 1) \tag{5}$$

where N and M are the nonlinearity order and the memory depth of the polynomial function, respectively.

The total size of the model, quantified in terms of the number of complex-valued coefficients needed to implement the full predistortion function, is given by:

$$\begin{aligned} Size_{\text{Proposed}} &= Size_{Poly} + \frac{K}{2} \\ Size_{\text{RTNTB}} &= Size_{Poly} + K \\ Size_{\text{EMP}} &= Size_{Poly} \end{aligned} \tag{6}$$

where K is the nonlinearity order of the static distortions function as defined in Eq. (3).

Figure 7 presents the NMSE results of the DPD identification as a function of the memory polynomial number of coefficients for the three considered DPDs (proposed, RTNTB, and EMP) with the 20MHz and 40MHz test signals. These results show that the proposed DPD consistently outperforms the EMP based DPD for the 20MHz and 40MHz test signals. Moreover, the proposed DPD has comparable accuracy to the RTNTB DPD for the 20MHz signal. However, when stronger memory effects are present (as it is the case with the 40MHz test signal), the proposed DPD can mimic the desired predistorted signal better than the RTNTB predistorter.

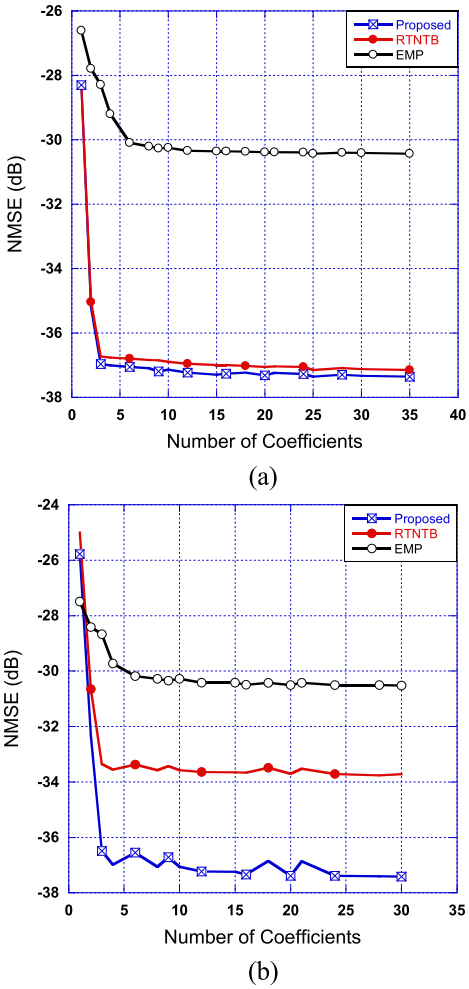

FIGURE 7. NMSE for DPD identification (a) 20MHz test signal, (b) 40MHz test signal.

The measured adjacent channel leakage ratio (ACLR) at the output of the linearized DUT as a function of the total size of the MP function are reported in Fig. 8. These results show that the performance of the proposed predistorter is similar to that of the RTNTB, and is superior to that of the EMP based predistorter. In fact, the proposed DPD achieves an ACLR of better than –50dBC in the adjacent channel, and –56dBC in the alternate adjacent channel with as low as 15 coefficients in the memory polynomial function. The RTNTB achieves comparable performance which is consistently 1 to 2dB worse than the proposed DPD. The EMP model seems to be unable to linearize the DUT at hand with the considered number of coefficients. A sample of the measured spectra at the output of the linearized amplifier is shown in Fig. 9. This figure clearly shows that with only 15 parameters in the MP function, the proposed predistorter achieves a quasi-perfect cancellation of the distortions at the output of the DUT.

The same tests were reproduced with the 40MHz 5G test signal. The measured ACLR data for each model as a function of the memory polynomial function size is summarized in Fig. 10. According to this figure, the proposed

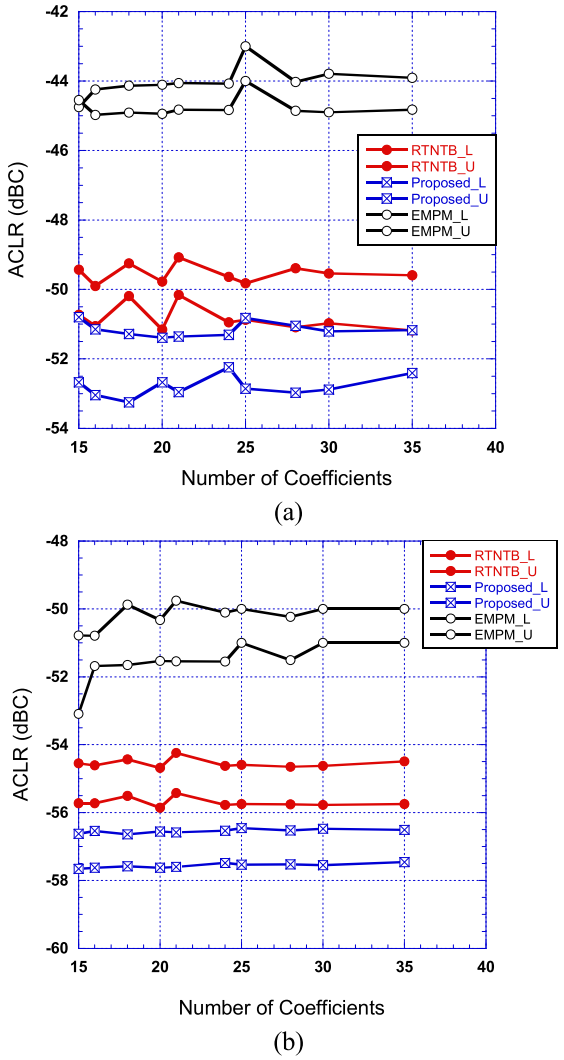

FIGURE 8. Measured ACLR for the 20MHz 5G test signal (a) ACLR1 upper and lower, (b) ACLR2 upper and lower.

model achieved an ACLR better than –50dBC with as low as 15 coefficients in the MP sub-function. Comparable results are obtained for the RTNTB model. However, it is clear that the EMP is unable to compensate for the strong memory effects and its performance in the adjacent channel is around –42dBC that is 10dB worse than the proposed model. Samples of the measured spectra at the output of the linearized DUT are depicted in Fig. 11. These spectra, corresponding to 15 coefficients in the MP function, show that there is no noticeable residual distortions at the output of the PA when the proposed DPD is applied. However, slight distortions remain un-compensated in the vicinity of the carrier with the RTNTB model. The EMP model is unable to linearize the proposed DUT under these conditions.

The results reported in this section clearly demonstrate the ability of the proposed model in achieving complete cancellation of the distortions at the output of the DUT while requiring a reasonably low number of coefficients. Moreover, it is important to highlight that the LUT is implemented as a

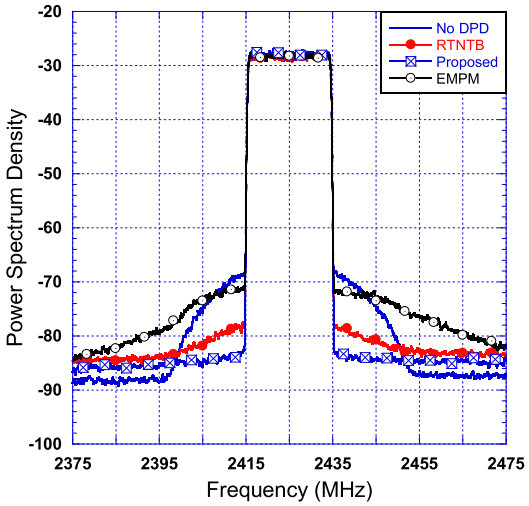

FIGURE 9. Measured spectra at the output of the linearized amplifier for a 20MHz 5G test signal (with 15 coefficients in the MP sub-functions).

memoryless polynomial function with $K = 12$ coefficients. Hence, in the case of the RTNTB model, the LUT implementation requires 12 complex-valued coefficients, while in that of the proposed DPD, the AM/AM LUT only requires 12 real-valued coefficients, which is a computational complexity equivalent to 6 complex-valued coefficients.

Accordingly for a memory polynomial function with 15 complex-valued coefficients in the proposed DPD, the total model size is equivalent to 21 complex-valued coefficients. However, for the same size of the memory polynomial function (that is 15 complex-valued coefficients), the RTNTB model size is equivalent to 27 complex-valued coefficients. Hence, while achieving comparable performance to the RTNTB, the proposed DPD leads to approximately 22% reduction in the model complexity (21 coefficients instead of 27). The results of Figures 8 and 10 show that for the case of the EMP model, the performances in terms of ACLR cannot reach a level comparable to that of the proposed and RTNTB DPDs even if the model size is increased up to 35 complex-valued coefficients.

Based on the results of the two test signals, it appears that the proposed DPD outperforms the EMP model. Moreover, the proposed DPD performance presents a slight enhancement compared to the RTNTB model. However, the superiority of the proposed DPD (when compared to the RTNTB model) resides in its complexity reduction (in terms of number of coefficients) which is in the range of 20%. Furthermore, as it will be discussed in the next section, the proposed model is more suitable than the RTNTB model for hybrid baseband/RF implementation, and can allow for substantial benefits in terms of digital to analog converter speed.

IV. PROPOSED DPD IMPACT ON THE TRANSMIT PATH DAC SPEED

Conceptually, the proposed DPD and the RTNTB DPD can be implemented either using the architecture of Fig. 3 or

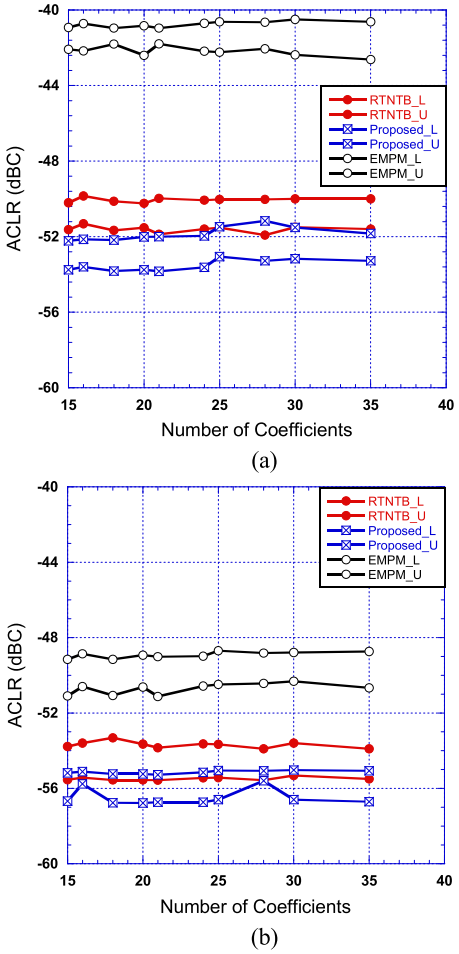

FIGURE 10. Measured ACLR for the 40MHz 5G test signal (a) ACLR1 upper and lower, (b) ACLR2 upper and lower.

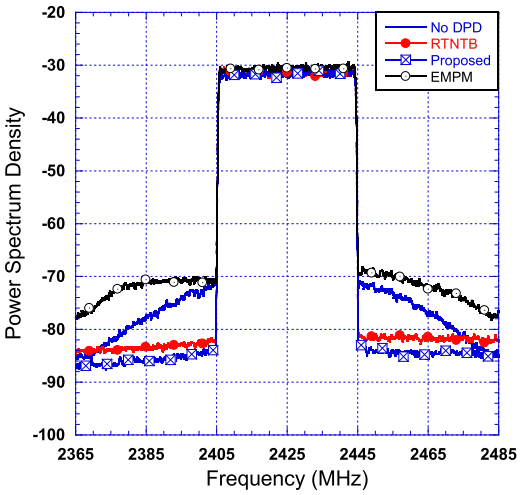

FIGURE 11. Measured spectra at the output of the linearized amplifier for a 40MHz 5G test signal (with 15 coefficients in the MP sub-functions).

that of Fig. 4. However, a major drawback of the RTNTB predistorter that hinders its hybrid implementation is due to the fact that the analog implementation of the memoryless predistortion function is complex. Indeed, it requires applying power dependent magnitude and phase corrections on the RF signal. The proposed DPD addresses this issue by simplifying the memoryless predistortion function and reducing it to just a power dependent gain/attenuation function. By enabling a low complexity hybrid implementation, the proposed DPD can relax the speed requirements on the DAC of the transmit path.

To illustrate this aspect, the intermediate spectra for the predistorters used to achieve the linearization performance reported in Figures 9 and 11 were derived. Fig. 12 and Fig. 13 report the spectra for the case of the 20MHz and 40MHz 5G test signals, respectively. Each of these figures includes the spectra at the output of the MP sub-function (MP node) of both the proposed and the RTNTB predistorters. The fully predistorted signal (output of the predistorter) is also included for the proposed, the RTNTNB and the EMP predistorters. Figures 12 and 13 clearly show that the partly predistorted signals at the output of the MP sub-function do not present any significant spectrum regrowth and have a bandwidth similar to that of the input signal. This is due to the fact that the partly predistorted signal at the output of the MP sub-function has been subject to a mildly nonlinear function which does not result in noticeable spectrum regrowth in the adjacent channel. Conversely, the fully predistorted signals have significant spectrum regrowth in the adjacent channels. In fact, typically a fully predistorted signal spans over 5 times the bandwidth of the original signal. Hence, applying the digital to analog conversion on the partly predistorted signal at the output of the MP sub-function can lead to significant reduction, of up to 80%, in the predistorted signal bandwidth at the DAC input. This will in turn result in a proportional reduction in the DAC speed requirements for the transmit path, which will also lead to lower power consumption for the DAC block.

It is worthy to mention here that the EMP DPD is also suitable for RF implementation. In such case, the signal at the input of the transmit path's DAC will simply be the non-predistorted input signal which has a bandwidth comparable to that of the DAC's input signal in the hybrid implementation of the proposed DPD. However, as illustrated in the previous section, the proposed DPD achieves superior performance in terms of spectrum regrowth cancellation. Accordingly, the proposed DPD system outperforms the RTNTB model in terms of number of coefficients and ease of implementation in a hybrid configuration to relax the DAC speed requirements, while achieving comparable performance. Furthermore, it outperforms the EMP DPD in terms of performance and ease of implementation in a hybrid configuration for a comparable benefits in terms of DAC speed requirements.

To further validate the ability of the proposed model in reducing the operating sampling rate of the digital to analog converter, the hybrid implementation of Fig. 4 was considered. Since the implementation of the analog LUT is out of the

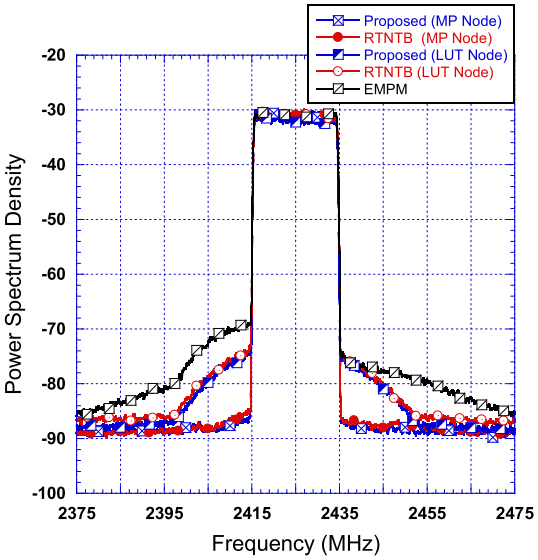

FIGURE 12. Measured spectra of the predistorted signal at various nodes of the DPD for a 20MHz 5G test signal (with 15 coefficients in the MP sub-functions).

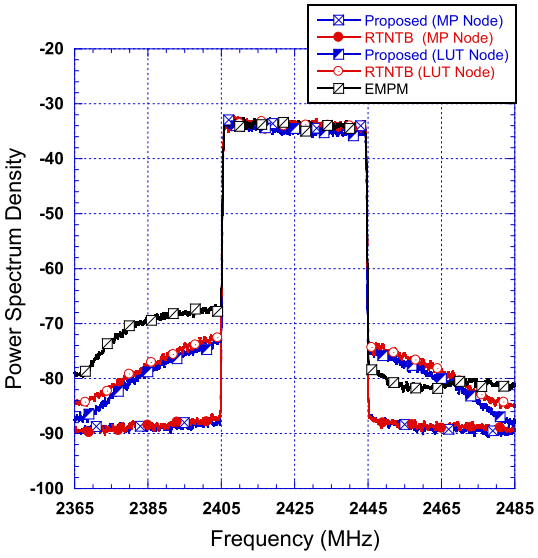

FIGURE 13. Measured spectra of the predistorted signal at various nodes of the DPD for a 40MHz 5G test signal (with 15 coefficients in the MP sub-functions).

scope of this work, the following test scenario was performed. First, the DUT characteristics were acquired, and the two sub-functions of the proposed DPD were synthesized. The signal at the output of the MP sub-function was downloaded into the signal generator and the corresponding analog signal generated at reduced sampling rates. The digital to analog conversion of the partly predistorted signal was performed at 40.96Msps and 51.2Msps for the 20MHz and the 40MHz test signals, respectively. To mimic the memoryless LUT, the partly predistorted signal was acquired again and applied to the memory LUT (which was digitally implemented in this case). Fig. 14 reports the measured spectra at the output of the linearized amplifier obtained from this test condition (hybrid implementation). These results are also compared to the fully

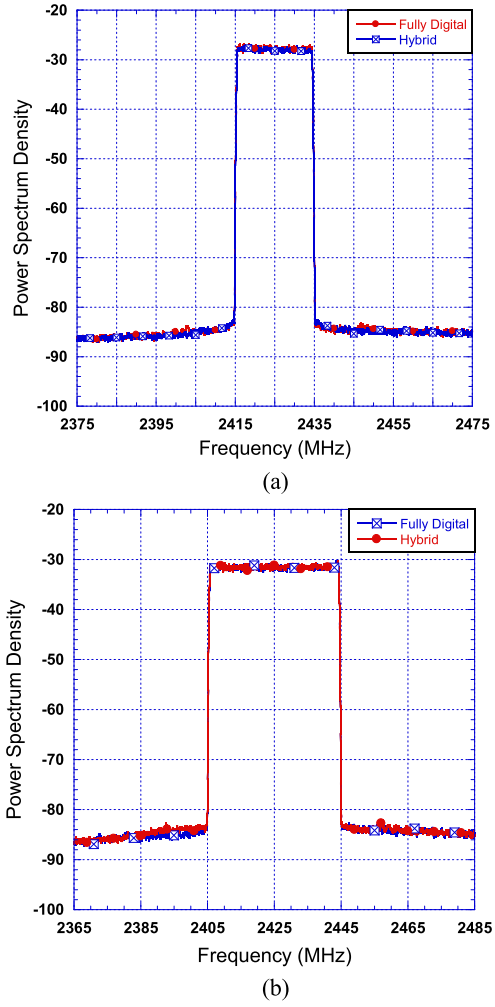

FIGURE 14. Measured spectra at the output of the linearized amplifier using the fully digital and hybrid implementations of the proposed DPD (a) 20MHz 5G test signal, (b) 40MHz 5G test signal.

digital implementation of the proposed predistorter. This figure shows that for both test signals, the proposed predistorter performance is not affected by the hybrid implementation involving low-speed digital to analog conversion.

V. CONCLUSION

In this paper, a novel digital predistorter was proposed. This predistorter was derived with the objectives of achieving high performance, while being suitable for low-complexity hybrid implementation in order to enable relaxed sampling rates in the transmit path of digital predistortion systems. The proposed DPD was experimentally validated using 20MHz and 40MHz 5G test signals on a commercial GaN PA evaluation board. The proposed DPD was found to achieve better than –50dBC ACLR performance with a reasonably low number of coefficients. Compared to benchmark models, the proposed DPD achieves comparable performance to the RTNTB model while reducing by more than 25% the total number of coefficients. Moreover, it also reduces by approximately 80% the bandwidth requirements of the DAC used in the transmit path.

The proposed model can be efficiently implemented in hybrid baseband digital and RF analog predistortion systems to allow for memory effects compensation with low complexity and high performance.

DISCLAIMER

This paper represents the opinions of the author(s) and does not mean to represent the position or opinions of the American University of Sharjah.

REFERENCES

[1] F. M. Ghannouchi, O. Hammi, and M. Helaoui, *Behavioral Modeling and Predistortion of Wideband Wireless Transmitters*. Hoboken, NJ, USA: Wiley, 2015.
[2] T. Qi and S. He, "Power up potential power amplifier technologies for 5G applications," *IEEE Microw. Mag.*, vol. 20, no. 6, pp. 89–101, Jun. 2019.
[3] A. Katz, J. Wood, and D. Chokola, "The evolution of PA linearization: From classic feedforward and feedback through analog and digital predistortion," *IEEE Microw. Mag.*, vol. 17, no. 2, pp. 32–40, Feb. 2016.
[4] F. M. Ghannouchi and O. Hammi, "Behavioral modeling and predistortion," *IEEE Microw. Mag.*, vol. 10, no. 7, pp. 52–64, Dec. 2009.
[5] J. Kim and K. Konstantinou, "Digital predistortion of wideband signals based on power amplifier model with memory," *Electron. Lett.*, vol. 37, no. 23, pp. 1417–1418, Nov. 2001.
[6] D. R. Morgan, Z. Ma, J. Kim, M. G. Zierdt, and J. Pastalan, "A generalized memory polynomial model for digital predistortion of RF power amplifiers," *IEEE Trans. Signal Process.*, vol. 54, no. 10, pp. 3852–3860, Oct. 2006.
[7] O. Hammi, F. M. Ghannouchi, and B. Vassilakis, "A compact envelope-memory polynomial for RF transmitters modeling with application to baseband and RF-digital predistortion," *IEEE Microw. Wireless Compon. Lett.*, vol. 18, no. 5, pp. 359–361, May 2008.
[8] O. Hammi and F. M. Ghannouchi, "Twin nonlinear two-box models for power amplifiers and transmitters exhibiting memory effects with application to digital predistortion," *IEEE Microw. Compon. Lett.*, vol. 19, no. 8, pp. 530–532, Aug. 2009.
[9] T. Liu, S. Boumaiza, and F. M. Ghannouchi, "Augmented Hammerstein predistorter for linearization of broad-band wireless transmitters," *IEEE Trans. Microw. Theory Techn.*, vol. 54, no. 4, pp. 1340–1349, Jun. 2006.
[10] P. L. Gilabert, G. Montoro, and E. Bertran, "On the Wiener and Hammerstein models for power amplifier predistortion," in *Proc. Asia–Pacific Microw. Conf.*, Dec. 2005, pp. 1–4.
[11] T. Kobal, Y. Li, X. Wang, and A. Zhu, "Digital predistortion of RF power amplifiers with phase-gated recurrent neural networks," *IEEE Trans. Microw. Theory Techn.*, vol. 70, no. 6, pp. 3291–3299, Jun. 2022.
[12] M. Tanio, N. Ishii, and N. Kamiya, "Efficient digital predistortion using sparse neural network," *IEEE Access*, vol. 8, pp. 117841–117852, 2020.
[13] H. Li, Y. Zhang, G. Li, and F. Liu, "Vector decomposed long short-term memory model for behavioral modeling and digital predistortion for wideband RF power amplifiers," *IEEE Access*, vol. 8, pp. 63780–63789, 2020.
[14] Y. Zhang, Y. Li, F. Liu, and A. Zhu, "Vector decomposition based time-delay neural network behavioral model for digital predistortion of RF power amplifiers," *IEEE Access*, vol. 7, pp. 91559–91568, 2019.
[15] *3GPP Specification Series: 38Series*. 3GPP. Accessed: Jun. 3, 2022. [Online]. Available: https://www.3gpp.org/DynaReport/38-series.htm
[16] Y. Liu, W. Pan, S. Shao, and Y. Tang, "A new digital predistortion for wideband power amplifiers with constrained feedback bandwidth," *IEEE Microw. Wireless Compon. Lett.*, vol. 23, no. 12, pp. 683–685, Dec. 2013.
[17] Y. Ma, Y. Yamao, Y. Akaiwa, and K. Ishibashi, "Wideband digital predistortion using spectral extrapolation of band-limited feedback signal," *IEEE Trans. Circuits Syst. I, Reg. Papers*, vol. 61, no. 7, pp. 2088–2097, Jul. 2014.
[18] A. B. Ayed, E. Ng, P. Mitran, and S. Boumaiza, "Digital predistortion of millimeter-wave hybrid beamforming transmitters using observation receivers with low-bit resolution analog-to-digital converter," *IEEE Access*, vol. 9, pp. 100627–100636, 2021.
[19] E. G. Jeckeln, F. M. Ghannouchi, and M. A. Sawan, "A new adaptive predistortion technique using software-defined radio and DSP technologies suitable for base station 3G power amplifiers," *IEEE Trans. Microw. Theory Techn.*, vol. 52, no. 9, pp. 2139–2147, Sep. 2004.
[20] S. Boumaiza, J. Li, M. Jaidane-Saidane, and F. M. Ghannouchi, "Adaptive digital/RF predistortion using a nonuniform LUT indexing function with built-in dependence on the amplifier nonlinearity," *IEEE Trans. Microw. Theory Techn.*, vol. 52, no. 12, pp. 2670–2677, Dec. 2004.
[21] A. Kumar and M. Rawat, "Adaptive dual-input analog RF predistorter for wideband 5G communication systems," *IEEE Trans. Circuits Syst. I, Reg. Papers*, vol. 68, no. 11, pp. 4636–4647, Nov. 2021.
[22] J. Xia, A. Islam, H. Huang, and S. Boumaiza, "Envelope memory polynomial reformulation for hardware optimization of analog-RF predistortion," *IEEE Microw. Wireless Compon. Lett.*, vol. 25, no. 6, pp. 415–417, Jun. 2015.
[23] O. Hammi, F. M. Ghannouchi, S. Boumaiza, and B. Vassilakis, "A data-based nested LUT model for RF power amplifiers exhibiting memory effects," *IEEE Microw. Wireless Compon. Lett.*, vol. 17, no. 10, pp. 712–714, Oct. 2007.
[24] A. I. Dalbah, O. Hammi, and A. Zerguine, "Hybrid look-up-tables based behavioral model for dynamic nonlinear power amplifiers," *IEEE Access*, vol. 8, pp. 53240–53249, 2020.

ANFAL ALSAYED ALI received the B.S. (cum laude) and M.S. degrees in electrical engineering from the American University of Sharjah, Sharjah, United Arab Emirates, in 2018 and 2021, respectively. From 2019 to 2021, she was a Research Assistant at the American University of Sharjah. Her research interests include machine learning, neural networks, behavioral modeling, and linearization of radio frequency power amplifiers.

SERIEN AHMED received the B.S. degree in electrical and electronic engineering with a minor in control and instrumentation from the University of Khartoum, Sudan, in 2017. She is currently pursuing the M.S. degree with the American University of Sharjah, United Arab Emirates. Her current research interests include the design of linear wireless transmitters, relaxed sampling rate predistorters, and digital signal processing.

OUALID HAMMI (Member, IEEE) received the B.Eng. degree from the École Nationale d'Ingénieurs de Tunis, Tunis, Tunisia, in 2001, the M.Sc. degree from the École Polytechnique de Montréal, Montréal, QC, Canada, in 2004, and the Ph.D. degree from the University of Calgary, Calgary, AB, Canada, in 2008, all in electrical engineering.

From 2010 to 2015, he was a Faculty Member of the Department of Electrical Engineering, King Fahd University of Petroleum and Minerals, Dhahran, Saudi Arabia. He is currently a Professor with the Electrical Engineering Department, American University of Sharjah, Sharjah, United Arab Emirates. He is the coauthor of two books, more than 100 articles, and inventor/co-inventor on 13 U.S. patents. His research interests include the design of energy-efficient linear transmitters for wireless communication and satellite systems and the characterization, behavioral modeling, and linearization of radiofrequency power amplifiers and transmitters.